SMiRT-12 / K. Kussmaul (Editor)

H09/5

LOADING CAPACITIES AND FAILURE MODES OF VARIOUS REINFORCED CONCRETE SLABS SUBJECTED TO HIGH-SPEED LOADING

H. Saito[1], A. Imamura[1], M. Takeuchi[1], S. Okamoto[2], Y. Kasai[3], H. Tsubota[3] and M. Yoshimura[4]

[1]Tokyo Electric Power Co., Tokyo, [2]Ohsaki Research Institute, Inc., Tokyo, [3]Kobori Research Complex, Inc., Tokyo, [4]Tajimi Engineering Services Ltd., Tokyo (Japan)

Abstract

The objective of this study was to clarify experimentally and analytically the loading capacities, deformations and failure modes of various types of reinforced concrete structures subjected to loads applied at various loading rates. Flat slabs, slabs with beams and cylindrical walls were tested under static, low-speed and high-speed loading. Analysis was applied to estimate the test results by the finite element method using a layered shell element. The analysis closely simulated the experimental results until punching shear failure occurred.

1 Introduction

Nuclear power plant buildings are subjected to external loads at various loading rates, for example static loads, seismic loads and impact loads. The characteristic of the hysteresis curve for reinforced concrete structures, expressed by the relationship between load and response deformation, greatly varies depending on the structural deformation rate.

A high-speed loading apparatus was used to apply concentrated loads to the surface of approximately 1/7.5 scale models of seven types of reinforced concrete plates used for industrial facilities. Three loading speeds were used: static, low-speed and high-speed. Thus, the relationship between loading rate and loading capacities, and the degree of deformation were clarified. Part of this study was published in reference /1/.

The behavior of typical specimens was analyzed by applying the finite element method, taking into account dynamic loading, the non-elasticity of materials and cracks in the concrete. It was noted how the characteristics of hysteresis curve were affected by the loading rate.

2 EXPERIMENTAL METHOD AND SPECIMEN

Figure 1 shows the shapes of the test specimens. Table 1 shows the basic configurations of the seven types of test specimens. The flat-slab test specimens were simply supported on all four sides at 100 cm span positions. Slabs in specimen D and E were the same as that in specimen C. In specimen.E, a steel beam was connected to the slab by shear studs. In the cylindrical wall test specimens, a curved plate measuring 150 cm x 100 cm in the shape of a part of a cylindrical wall, was simply supported on two sides at 120 cm span positions. To prevent deformation by circumferential expansion, the two sides of the curved plate were constrained elastically by PC steel bars.

Using the high-speed loading apparatus shown in Figure 2, the test specimen was loaded with a square steel loading plate, 15 cm x 15 cm and 5 cm thick, placed in contact with the center of the test specimen. (/2/ Tsujimoto 1989)

The loading plate could be moved at any selected speed by dislocating the actuator up to the apparatus capacities of 15 cm-displacement. The setting speeds during the test were 3.0 m/s for high-speed loading, 0.03 m/s for low-speed loading and 3.0^{-5}m/s for static loading.

3.MATERIAL TEST

To assess the mechanical properties of the test specimen material, material tests were conducted at static, low-speed, and high-speed loadings. Table 2 shows test results of the compressive strength and tensile strength of the concrete material. The test was conducted on 10 cm-diameter cylinders. Young's modulus was evaluated with a secant elastic modulus at the 1/3 point of the stress level for the compressive strength.

Table 2 also shows the tensile test results for the reinforcing bar (D10) used as the main reinforcement for the test specimens.

4 TEST RESULTS

Bending deformation occurred in the flat slab during the initial loading stage in all the loading tests, and in the final stage punching shear failure resulted. The final failure modes were nearly the same for all loading rates. That is, no cracks appeared in the front surface of the specimens except for the hole drilled with the loading plate; however, cracks radiated from the rear surface.(/1/ Saitoh 1992)

Figure 3 and Figure 4 respectively show the final failure conditions of the cylindrical wall test specimens after static and high-speed loading tests. The failure modes were greatly affected by the loading rates. During static loading, punching shear failure occurred. On the other hand, bending compression failure occurred during high-speed loading and the specimen cracked at the center. Punching shear failure was observed on the rear surface at the final loading stage as indicated in Figure 4.

The steel beams had local buckling failure mode in both slab specimens and beam specimens.

Table 3 shows the maximum strength of each specimen. Figures 5 to 11 show the relationship between the load and the displacement at the loading point at the center of the test specimen.

In every test specimen, the maximum strength increased in the order of static, low-speed, and high-speed loading, indicating that the greater the loading rate, the greater the load that could be borne by the structural components. This is due to the fact that the compressive strengths and tensile strengths of the concrete and reinforcing bars increase with the loading rate, as indicated by the results of the material test.

The effect of these parameters on maximum strength is described below:

Slab thickness: In the test on flat slab (A), which was 12 cm thick, the maximum strength was 7% greater during low-speed loading and 35% greater during high-speed loading than during static loading. Also, in the test of 7 cm thick flat slab (C), with the same reinforcement ratio, the maximum strength was 14% greater during low-speed loading and 71% greater during high-speed loading than during static loading. Thus, it can be concluded that the increase in maximum strength for the flat slab (C) was twice that of the flat slab (A).

Reinforcement ratio: A comparison of flat slabs (A) and (B), in which only the reinforcement ratio was different, indicates that the increase in maximum strength is nearly the same in (A) and (B) for both low-speed and high-speed loading. It may be concluded, therefore, that the reinforcement ratio hardly affects the maximum strength when the loading rate increases.

Beam: The increase in strength of the slabs with the RC beam were similar to that of the flat slabs.

The combined strengths of the slabs with the steel beam during all loadings were greater than the sum of the individual strengths. The local buckling of the steel beam in composite structure was less than for the steel beam by itself.

The increase in strength with loading speed is much less for the steel beam by itself than it is for all the other configurations.

Cylindrical wall: The maximum strength of the cylindrical wall specimen proved to be 44% greater during high-speed loading than during static loading. The experimental conditions for the cylindrical wall specimens were different from those for the flat-slab specimens in that a one way slab was used and an in-plane axial force was applied. Despite such differences, the increase in maximum strength was as great as it was in the flat-slab specimens.

5 ANALYTICAL SIMULATION OF TEST RESULTS

Simulation analyses were conducted on typical test specimen using a nonlinear finite element analysis program using the layered shell elements shown in Figure 12 (/3/ Uchida 1985). Reference /1/ reported good analytical results for the flat-slab(C). This paper presents analyses on the cylindrical wall specimen. It is difficult to simulate punching shear failure during static loading shown in Figure 3 with layered shell element. The analysis was applied to the test case during high-speed loading in which bending failure mode was observed as shown in Figure 4.

As Figure 14 shows the analysis model, a flat quadrilateral element was adopted to model a quarter part of the specimen for which symmetry was considered. The concrete was partitioned into 63 elements and 7 layers, and the reinforcement was modeled by equivalent layers with rigidity in only the reinforcement direction. For the analyses, the stress-strain relationships for the concrete and reinforcing bars under high-speed conditions were assumed to be as shown in Figure 13, based on the material test results. The PC steel bar was modeled by a rod element.

During high-speed loading, the load-time relation was measured as a reaction force at the loading plate, shown by the solid line in Figure 15. As shown, two load cases were assumed as the external load representing the reaction force. Real time-load relation curve was roughly smoothed in Case A and more exactly smoothed in Case B.

Then a nonlinear analysis for the time-dependent load was performed to calculate the responses. The analyzed results were compared with the experimental results. The solid line in Figure 16 shows the relationship between the load and the displacement at the center of the test specimen, obtained through the experiments so that the results of both cases could be compared.

Figure 16 shows that the experimental results and the analytical results match well. Thus, in nonlinear finite element analysis of reinforced concrete structures using layered shell elements, once the material characteristics

for each loading are given, it is possible to explain the experimental results until punching shear failure occurs. Figure 17 shows the deformed shape at maximum strength and the cracking distribution in Case B. By comparing Figure 17 and Figure 4, it can be seen the cracking distribution determined from this analysis is similar to the failure mode obtained by the experiment.

6 CONCLUSIONS

By applying concentrated loads to the surface of reinforced concrete slabs at static, low, and high loading rates, we find that, as the loading rate increases, the deformation modes and the failure modes of slabs change, and the maximum strength of the slab increases.

We also find that the loading test results until the occurrence of punching shear failure can be explained by indicating the material characteristics at high speed loading by a nonlinear finite element analysis of the reinforced concrete structures using layered shell elements.

This study was carried out as a part of the joint research study by 10 electric power companies in Japan (Tokyo, Hokkaido, Tohoku, Chubu, Hokuriku, Kansai, Chugoku, Shikoku, Kyushu and Japan Atomic).

REFERENCES

/1/ Saito,H., Imamura,A., Takeuchi,M., Kasai,Y., Okamoto,S. and Yoshimura,M. 1992. "Loading tests and analyses of various types of reinforced concrete slabs under different deformation speeds" Proceedings of the 10th World Conference on Earthquake Engineering Vol.6 : 3117 - 3120

/2/ Tsujimoto,M., Takahashi,Y., Ohno,T. and Uchida,T. 1989. "Dynamic properties and ultimate capacities of reinforced concrete slabs subjected to high-speed loading." Journal of Structural Engineering Vol. 35A, Japan Society of Civil Engineers : 1081- 1094

/3/ Uchida,T., Tsubota,H. and Yamada,T. 1985. "Experimental investigation on reinforced concrete slabs subjected to impact loading." Transactions of the 8th International Conference on Structural Mechanics in Reactor Technology J5/1 : 173-178

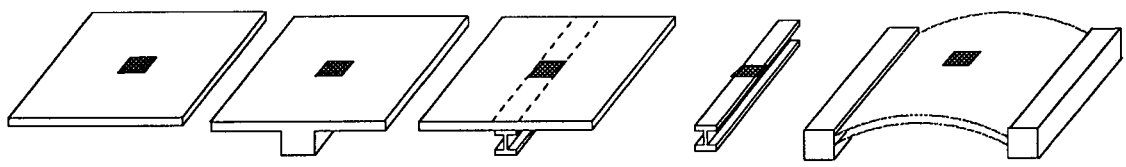

Flat slab (A) - (C) Slab with RC beam Slab with steel beam Steel beam Cylindrical wall

Figure 1. Shapes of test specimens

Table 1. Test specimens and loading rate O : tested

No	Types of specimen	Specimen dimensions (mm)	Slab Thick-ness (mm)	Slab Rebar ratio	Loading rate		
					Static	Low	High
					$3x10^{-5}$m/s	$3x10^{-2}$m/s	3m/s
A	Flat slab(A)	1200 x 1200	120	0.5%	O	O	O
B	Flat slab(B)	1200 x 1200	120	0.2%	O	O	O
C	Flat slab(C)	1200 x 1200	70	0.5%	O	O	O
D	Slab with RC-Beam	1200 x 1200 (B150xD200)	70	0.5%	O	O	O
E	Slab with Steel-Beam	1200 x 1200 (H-100x75)	70	0.5%	O	O	O
F	Steel-Beam	H-100x75x5x7	-	-	O	O	O
G	Part-cylindrical wall	1500 x 1000	90	0.4%	O	-	O

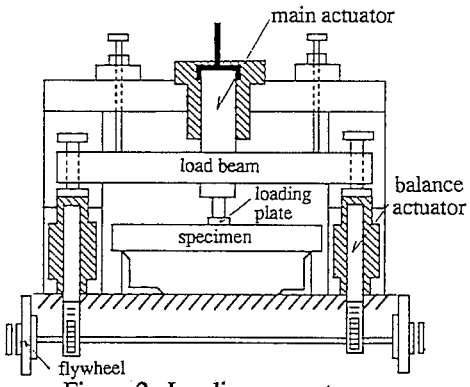

Figure 2. Loading apparatus

Table 2. Physical properties of concrete Unit: MPa

Material			Static	Low Speed	High Speed
Concrete	Flat slab	Compression	24.1	30.5	43.9
		Tension	2.0	2.8	5.9
		Young's modulus	21000	32100	42400
	Cylind-rical wall	Compression	33.0	-	51.0
		Tension	2.7	-	6.4
		Young's modulus	21300	-	43200
Reinforcing bar (SD295)		Yield Strength	367	423	445
		Tensile Strength	577	607	646

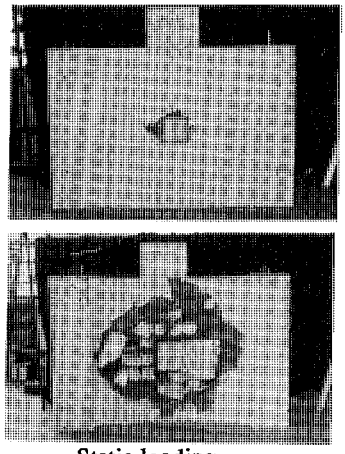

Static loading

Figure 3. Final failure of part-cylindrical wall

Table 3. Maximum strength of specimens Unit: kN

	Static	Low speed	High-speed
Flat slab(A)	174.0 (1.00)	186.6 (1.07)	234.8 (1.35)
Flat slab(B)	118.0 (1.00)	124.3 (1.05)	165.8 (1.41)
Flat slab(C)	61.7 (1.00)	70.2 (1.14)	105.6 (1.71)
Slab with RC-Beam	109.8 (1.00)	129.9 (1.18)	168.6 (1.54)
Slab with Steel-Beam	334.4 (1.00)	339.1 (1.01)	428.7 (1.44)
Steel-Beam	227.4 (1.00)	242.1 (1.06)	242.8 (1.07)
Part-cylindrical wall	201.4 (1.00)		289.7 (1.44)

Parentheses indicate the ratio of the value to the static loading test results

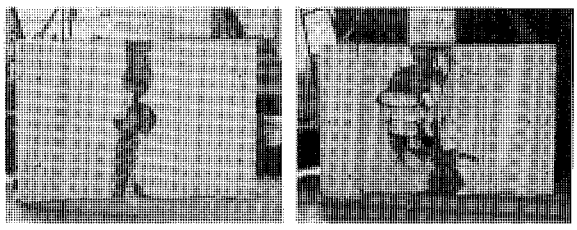

Front Rear

High-speed loading

Figure 4. Final failure of part-cylindrical wall

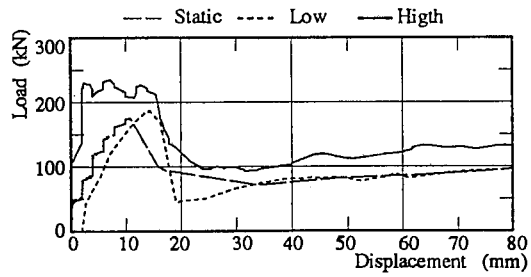

Figure 5. Load-displacement Curve (Flat slab A)

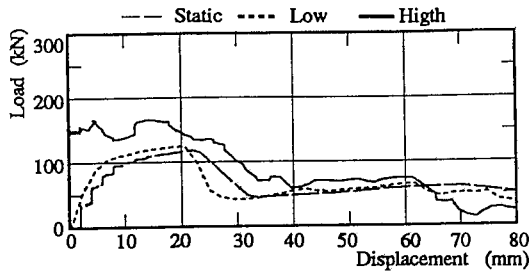

Figure 6. Load-displacement Curve (Flat slab B)

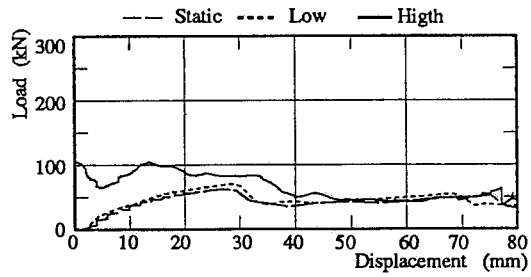

Figure 7. Load-displacement Curve (Flat slab C)

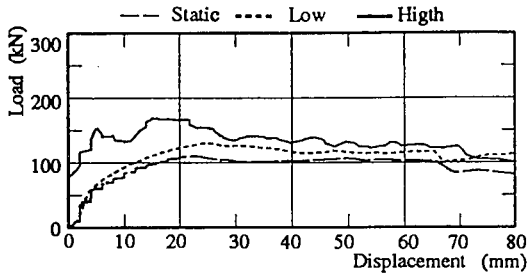

Figure 8. Load-displacement Curve(Slab with RC beam)

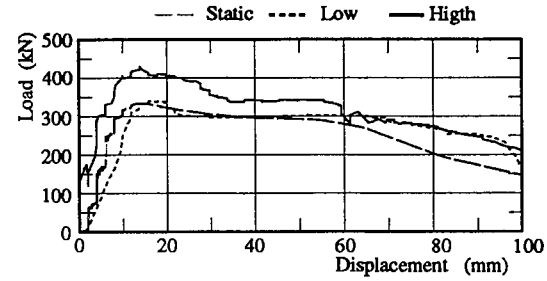

Figure 9. Load-displacement Curve(Slab with S beam)

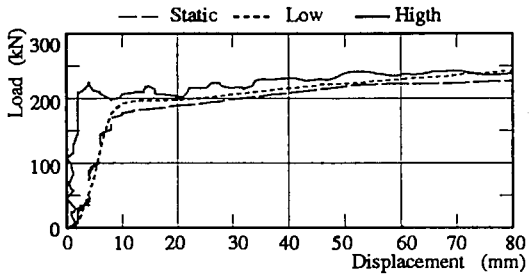

Figure 10. Load-displacement Curve(Steel beam)

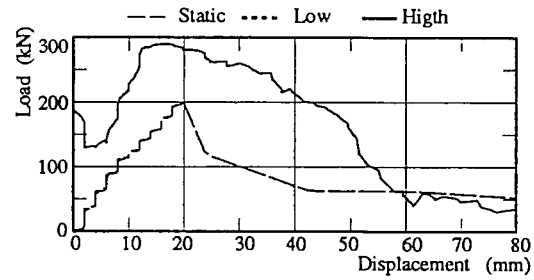

Figure 11. Load-displacement Curve (Cylindrical wall)

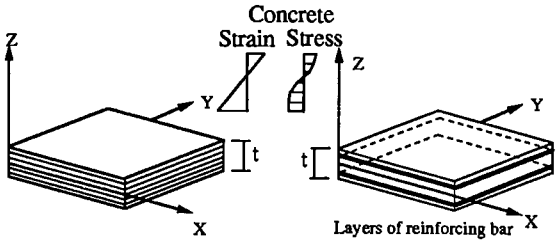

Figure 12. Layered shell element

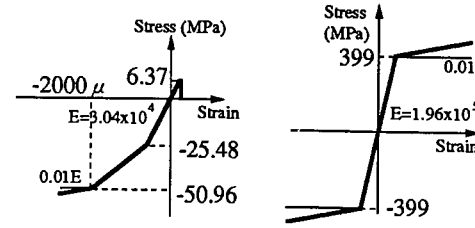

(a) Concrete (b) Reinforcing bar

Figure 13. Stress-strain curves for materials

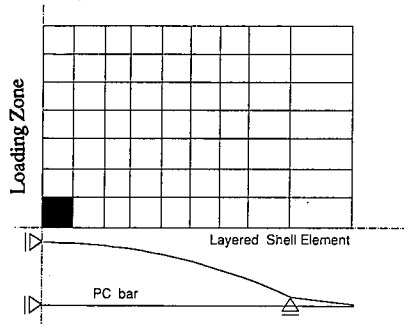

Figure 14 Analytical model of cylindrical wall

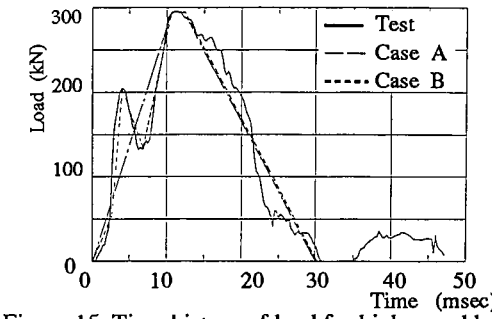

Figure 15. Time history of load for high speed loading

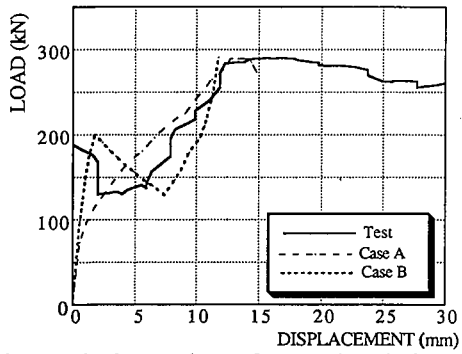

Figure 16. Comparison of test and analytical results

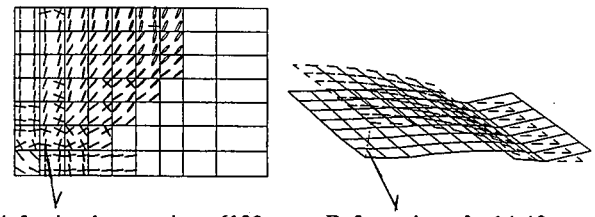

Reinforcing bar strain = 6120 μ Deformation δ =14.42mm

Crack distribution on rear surface At maximum load(12.8msec)

Case B

Figure 17. Cracks and Deformed shape at 12 ms